2018 26th Mediterranean Conference on Control and Automation (MED)
Zadar, Croatia, June 19-22, 2018

Combined Design of Adaptive Sliding Mode Control and Disturbance Observer with Friction Compensation for a Feed Drive System

Abdallah Farrage[1,2] and Naoki Uchiyama[2]

***Abstract*— Mechanical friction and disturbance are the key issues in precision control of mechanical systems especially in computer numerical controlled (CNC) feed drives. The friction does not only deteriorate the motion accuracy but also increases consumed energy of machining process. Feed drives have diverse applications and operate for a long time over the world, and therefore energy saving is highly expected. This paper proposes a combined design of adaptive sliding mode control and disturbance observer with a nonlinear static friction compensation to improve the motion accuracy and save consumed energy of a biaxial feed drive system. The friction compensator is designed based on a nonlinear friction model. Contour error, which is defined as the shortest distance between the actual position and the reference trajectory, is more important on the machining accuracy than the tracking error in each axis, and therefore contouring controllers are designed by feeding back contour errors. The disturbance observer and friction compensator are integrated into sliding mode contouring control and adaptive sliding mode contouring control. In order to verify the effectiveness of the combined design, comparative experiment was carried out with a biaxial feed drive system. The proposed approach effectively improved the contouring performance and achieved a significant reduction of the consumed energy.**

I. INTRODUCTION

Friction is one of the main factors which restricts producing highly accurate products and increases consumed energy in mechanical systems such as computer numerical control (CNC) machines [1]. Because of the nonlinear frictional behavior on machine tool feed drives, friction compensator is not easy to be experimentally implemented [2], [3]. Regarding to the friction model usage, the friction compensators are divided into two categories [4]. First, model free methods that consider the friction as a general disturbance. For example, Chih et al. introduced an observer based on a variable structure controller to overcome friction deficiencies [5]. Carl and Kobayashi proposed a zero phase error tracking controller with a disturbance observer [6]. Second, model based methods that apply extra driving force equivalent to the estimated friction force and can properly overcome the friction effects in a feed drive system [7], [8]. Several studies have confirmed the possibility of using the nonlinear friction compensation to improve the tracking accuracy. For example, Chih et al. formulated the dynamics of the nonlinear static friction and used particle swarm optimization (PSO) to tune disturbance parameters [9]. Alexander et al. proposed a feed forward friction compensation system for industrial applications [10].

In machine tool feed drive control, the contour error is more important than the tracking error because it directly relates to the shape of a final product. Several approaches are concerned with improving the machining accuracy based on the contouring performance [11]-[14]. However, the contouring control algorithm that considers only known dynamic parameters of the plant may deteriorate the response with unexpected friction and disturbance. Rafan et al. reduced the contour error for a ball screw driven stage using a friction compensator [15]. Uchiyama improved the contouring accuracy of a biaxial feed drive system using a nonlinear friction compensator [16]. Ba and Uchiyama achieved energy conservation for a three axis machine tool by applying the sliding mode control (SMC) with an adaptive friction compensator [17].

This paper is concerned with improving the contouring performance and the consumed energy of a biaxial feed drive system by conjunction the adaptive SMC (ASMC) and a disturbance observer with a nonlinear friction compensation. The proposed scheme was experimentally performed with a circular trajectory on a typical biaxial feed drive system. Results confirm the effectiveness of the proposed approach in improving the contouring accuracy and reducing consumed energy of feed drive systems compared to using only ASMC. The mean and maximum contour errors can be largely improved by 91.72% and 38.6%, respectively. The proposed approach can also reduce consumed energy by 0.898% and 2.05% for X and Y axis, respectively.

II. FRICTION IDENTIFICATION

A. Identification procedure

Friction compensation is employed to reduce contour errors. A typical biaxial mechanical system can be expressed by the following equation:

$$m_i \ddot{q}_i + d_i = f_i \qquad i = x, y \tag{1}$$

where m_i, q_i, d_i, and f_i are the table mass, table position, disturbance in the system including frictional sources, and the driving force for each axis, respectively. A proportional-derivative (PD) controller and a disturbance observer were implemented based on Eq. (1) to obtain values of friction coefficients. The driving force of the controller can be represented as follows:

$$f_i = m_i(\ddot{r}_i - k_{pi}\, e_i - k_{di}\, \dot{e}_i) + \hat{d}_i \tag{2}$$

*This work was not supported by any organization

[1]Abdallah Farrage is with Department of Mechanical Engineering, Toyohashi University of Technology, Toyohashi, 441-8580 Japan and assistant lecturer in Department of Mechanical Engineering, Faculty of Engineering, Assiut University, Assiut 71515, Egypt abdallahfraag@eng.au.edu.eg

[2]Department of Mechanical Engineering, Toyohashi University of Technology, Toyohashi, 441-8580 Japan uchiyama@tut.jp

978-1-5386-7891-6/18/$31.00 ©2018 IEEE

where r_i, k_{pi}, k_{di}, and $(e_i = q_i - r_i)$ are the desired position, proportional gain, derivative gain, and the tracking error, respectively. While, $\hat{d}_i$ is the estimated value of the friction force d_i. To obtain the friction force, the following disturbance observer was considered [7]:

$$\dot{\hat{v}}_i = \frac{1}{m_i}(f_i - \hat{d}_i) + k_{vi}(\hat{v}_i - \dot{r}_i) \tag{3}$$

$$\dot{\hat{d}}_i = k_{di}(\hat{v}_i - \dot{r}_i)$$

where k_{vi} and k_{di} are the disturbance observer gains and $\hat{v}_i$ is the estimated velocity.

B. Experimental setup

Experimental setup shown in Fig. 1 was employed to identify the friction model. The set up is a biaxial table driven by two DC servo motors. These motors are coupled with two ball screws. A rotary encoder with resolution 0.025 μm is attached to each motor to measure actual position for each feed drive axis. The program used to identify the friction parameters and control the biaxial feed drive system was written in C++ language using a personal computer (OS: Windows XP, CPU: 2 GHz) with a sampling time of 5 ms. To assure the same sampling time in a Windows XP environment, a timer on a 24-bit counter board is employed.

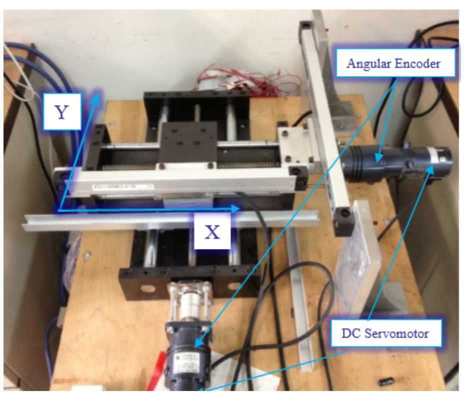

Fig. 1. Experimental Setup.

C. Identification result

The X axis in Fig. (1) was driven with a constant velocity to eliminate the inertia effect based on Eq. (1). The operated velocities are 0.01, 0.02, 0.04, 0.06, 0.08, 0.1, 0.2, 0.4, 0.6, 0.8, 1, 1.5, 2, 2.5, 3, 3.5, 4, 4.5, 5, 5.5, 6, 6.5, 7, 7.5, 8 mm/sec. The control and disturbance observer gains are k_p=3500 s^{-1}, k_d=150 s^{-2}, k_{ev}=50 s^{-1}, and k_{ed}=100 s^{-1}, respectively. The observed friction force was used to estimate the following friction coefficients.

$$f_f(\dot{q}_x) = \beta_1 \mathrm{sgn}(\dot{q}_x) + (\beta_2 - \beta_1)\mathrm{sgn}(\dot{q}_x)e^{-(\dot{q}_x v_o^{-1})^{\gamma}} + \beta_3 \dot{q}_x \tag{4}$$

where β_1, β_2, and β_3 are the Coulomb, static, and the viscous friction coefficients. γ and v_o are the parameters of Stribeck friction. The measured and fitted static friction model are illustrated in Fig. 2. The Stribeck effect was not obviously appeared in the experimental results, and it was assumed to be zero. The same experimental procedure was repeated for

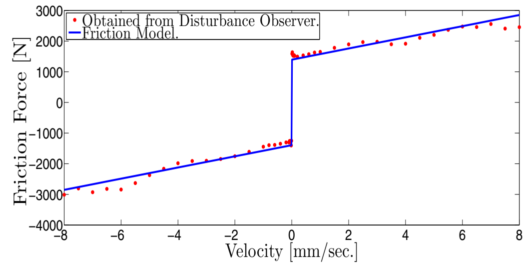

Fig. 2. Identification of Friction Model.

Y axis. The nonlinear static friction coefficients in Eq. (4) are experimentally obtained as for X axis; $\beta_1 = \beta_2 = 1257.20$ N, and $\beta_3 = 227.577$ Ns/mm and for Y axis; $\beta_1 = \beta_2 = 1106.85$ N, and $\beta_3 = 133.230$ Ns/mm.

III. Controller Design

The machining accuracy of CNC machines is directly influenced by the contour error because it is more important than the tracking error in each drive axis. In this paper, the friction compensator and disturbance observer were integrated into the contouring controller as follows:

$$f_{total} = f_c + f_f + f_d \tag{5}$$

where f_d and f_f are the estimated disturbance and the compensated friction forces calculated from Eqs. (3) and (4), respectively. f_{total} is the total driving force applied to the feed drive axes. f_c is the contouring control signal obtained from either SMC or ASMC. Because complicated computations are required to obtain the actual contour error in a complex trajectory case, It can be approximately estimated by considering Fig. 3, which shows the relationship between the tracking and the contour errors [19]. $\sum_w$ is the fixed coordinate frame with X and Y axes, and the tracking errors are described as follows:

$$e_w = [e_x, e_y]^T = q - r \tag{6}$$

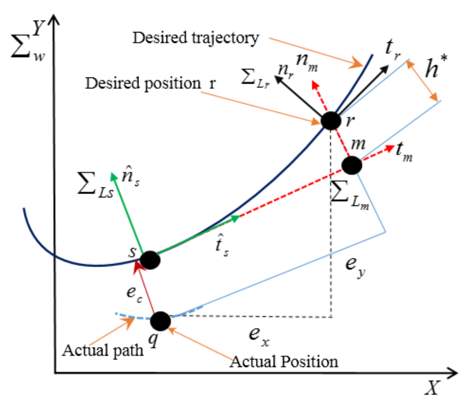

Fig. 3. Definition of Contour Error.

where $r = [r_x, r_y]^T$ and $q = [q_x, q_y]^T$. The contour error are represented by transforming the fixed frame $\sum_w$ to the desired position r. A frame $\sum_{L_r}$ with tangential and normal coordinates vectors (t_r, n_r) is represented as follows:

$$\begin{aligned} t_r = [t_{rx}, t_{ry}]^T &= \frac{\dot{r}}{\|\dot{r}\|}, \quad \|\dot{r}\| \neq 0. \\ n_r = [n_{rx}, n_{ry}]^T &= \frac{\dot{t}_r}{\|\dot{t}_r\|}, \ \|\dot{t}_r\| \neq 0. \end{aligned} \tag{7}$$

The transformed error on the desired point r with respect to $\sum_w$ can be expressed as follows:

$$\begin{aligned} e_{L_r} &= [e_{tr}, e_{nr}]^T = L_r^T e_w \\ L_r &= \begin{bmatrix} t_{rx} & n_{rx} \\ t_{ry} & n_{ry} \end{bmatrix} \end{aligned} \tag{8}$$

The normal component e_{nr} may be used as contour error. However, it may be inaccurate estimation especially in a high curvature motion. To effectively address this error, a point s was assumed on the desired trajectory whose distance to a point r equals the magnitude of tangential error e_{tr} approximately. The velocity along the segment (r-s) is also assumed to be constant and equal to the velocity at point r. Then the required time to traverse this segment t_d can be calculated as follows:

$$t_d = \frac{e_{tr}}{\|\dot{r}\|}, \quad \|\dot{r}\| \neq 0 \tag{9}$$

A new coordinate frame $\sum_{L_s}$ can be generated corresponding to the instantaneous time $t_s = t - t_d$ as follows:

$$\begin{aligned} \hat{t}_s &= [\hat{t}_{sx}, \hat{t}_{sy}]^T = t_r(t_s) \\ \hat{n}_s &= [\hat{n}_{sx}, \hat{n}_{sy}]^T = n_r(t_s) \end{aligned} \tag{10}$$

The transformed error with respect to $\sum_{L_s}$ can be assigned according to the new frame as follows:

$$\begin{aligned} e_{L_s} &= [e_{\hat{t}_s}, e_{\hat{n}_s}]^T = L_s^T e_w \\ L_s &= L_r(t_s) \end{aligned} \tag{11}$$

A frame $\sum_{L_m}$ is generated by transforming the frame $\sum_{L_s}$ to point m with tangential and normal components e_{t_m} and e_{n_m} as shown in Fig. 3 so that the final transformed error vector e_{L_m} is estimated as follows:

$$\begin{aligned} e_{L_m} &= [e_{t_m}, e_{n_m}]^T = L_s^T e_w + h^* \\ h^* &= [0, h_n^*] = J L_s^T [r(t_s) - r(t)] \end{aligned} \tag{12}$$

where $r(t_s)$ is the desired position of a feed drive at the time t_s and J is diag$\{0, 1\}$. The final normal error component e_{n_m} can be used to give a good estimation of actual contour error.

In this study, adaptive and nonadaptive SMC with a nonlinear sliding surface (NSS) [13] were implemented with the friction compensator and disturbance observer for a biaxial feed drive system shown in Fig. 1. The NSS is able to change the damping ratio with respect to the contouring performance and can be represented as follows:

$$S = [\lambda + \Phi\beta \ \ I] \begin{bmatrix} e_{L_m} \\ \dot{e}_{L_m} \end{bmatrix} = 0, \ \ S \in R^{2\text{x}1} \tag{13}$$

where $\lambda \in R^{2\text{x}2}$ is the linear term of sliding surface and has been chosen such that the dominant poles have small damping ratio and satisfies the Lyapunov equation $\beta\lambda^T + \lambda\beta = W$ for a positive definite matrix W. $\beta \in R^{2\text{x}2}$ is a positive definite matrix used to adjust the final damping ratio. $I \in R^{2\text{x}2}$ is the identity matrix. Φ is a diagonal matrix with positive diagonal elements which adjusts the damping ratio from its initial low value to a final high value. One possible choice of Φ is defined as follows [18]:

$$\Phi = \text{diag}\left\{\eta_i \frac{e^{-k_i e_i} + e^{k_i e_i}}{2}\right\} \tag{14}$$

$$e_i = \begin{cases} e_i & if \ |e_i| \leq e_{i\,max} \\ e_{i\,max}\text{sgn}(e_i) & if \ |e_i| > e_{i\,max} \end{cases} \quad i = t_m, n_m$$

where $e_{i\,max}$, η_i, k_i are positive tunning parameters used to adjust the maximum bound, minimum bound and variation rate of the magnitude $|\Phi|$, respectively. The first contouring controller (SMC) used in that study, can be defined as follows [19]:

$$\begin{aligned} f_c = M\Big\{\ddot{r} - L_s\Big[&(\lambda + \Phi\beta)\dot{e}_{L_m} + \ddot{L}_s^T e_w + 2\dot{L}_s^T \dot{e}_w \\ &+ \ddot{h}^* + \frac{d\Phi}{dt}\beta e_{L_m} + K_c S + Q\text{sgn}(S)\Big]\Big\} + C\dot{q} \end{aligned} \tag{15}$$

$$M = \text{diag}\{m_i\}, \ C = \text{diag}\{c_i\}, \ \ i = x, y$$

where c_i, is the equivalent viscous friction coefficient for the i^{th} axis. $K_c \in R^{2\text{x}2}$ is the constant diagonal gain matrix. sgn(S) is a 2x1 vector that includes the signs of each element of S, while $Q \in R^{2\text{x}2}$ is a diagonal matrix with diagonal elements chosen from the maximum bound of uncertainty as follows:

$$Q_i \geq \max(\widetilde{d}_i), \quad i = x, y \tag{16}$$

as $\widetilde{d}_i$ is an element of $(L_s^T M^{-1} d)$. Because of the constant control gain K_c in Eq. (15), the same ratio of energy was consumed over the running time regardless the contouring error magnitude. One possible attempt to reduce an excessive amount of consumed energy is the automatic tune of control gain depending on the resultant contour error. The adaptive law is chosen based on [20] and slightly modified to avoid the discontinuity function effects as follows:

$$K_c(t) = \int \rho\, S_m^2 \ dt \tag{17}$$

where ρ is a positive scalar of adaptation rate, and $S_m \in R^{2\text{x}2}$ is a diagonal matrix with diagonal elements of sliding surface values. The upper bound of control gain $K_c(t)$ was assigned to guarantee the system stability. Hence, the contouring controller proposed in that paper (ASMC) is presented as follows:

$$\begin{aligned} f_c = M\Big\{\ddot{r} - L_s\Big[&(\lambda + \Phi\beta)\dot{e}_{L_m} + 2\dot{L}_s^T \dot{e}_w + \ddot{L}_s^T e_w + \ddot{h}^* \\ &+ \frac{d\Phi}{dt}\beta e_{L_m} + K_c(t)\, S + Q\,\text{sgn}(S)\Big]\Big\} + C\dot{q} \end{aligned} \tag{18}$$

To minimize the effects of a discontinuity function in the previous two controllers, the following saturation function was considered.

$$\text{sat}(S) = \begin{cases} \text{sgn}(s_i) & if||s_i|| \geq \delta \\ \frac{s_i}{\delta} & if||s_i|| < \delta \end{cases} \qquad i = t_m, n_m \tag{19}$$

where δ is a positive scalar of boundary layer thickness, and s_i is the element of the sliding function S.

IV. Experimental Results

Experiments were conducted on a typical biaxial feed drive system shown in Fig. 1 using a circular trajectory. To assure fair comparison, the same initial condition and parameters shown in Table I were used. The control parameters have been chosen by trial and error in this study. The desired circular trajectory was assigned as follows:

$$x = 4\cos\left(\frac{\pi}{10}t\right) \text{ mm}, \quad y = 4\sin\left(\frac{\pi}{10}t\right) \text{ mm} \tag{20}$$

The actual contour error magnitude of each sampling time is determined as follows:

$$e_c(t_k) = \left| 4 - \sqrt{q_x(t_k)^2 + q_y(t_k)^2} \right| \quad \text{mm} \tag{21}$$

where t_k is the time at each sampling instant. In this study, the following algorithms were implemented with 1.256 mm/sec feed rate and compared:

- SMC in Eq. (15).
- SMC with a friction compensator and a disturbance observer (SMCFD) in Eq. (5).
- ASMC in Eq. (18).
- ASMC with a friction compensator and a disturbance observer (ASMCFD) in Eq. (5).

The experimental results of SMC and SMCFD are demonstrated in Figs. 4(a) and 4(b), respectively. The contouring and tracking performances of SMCFD have been significantly improved. The mean and maximum contour errors were largely reduced by 88.98% and 47.76% as shown in Figs. 5(a) and 5(b), respectively. The disturbance force and friction force based on a model in Eq. (4) for X and Y axes are shown in Figs. 6(a) and 6(b), respectively.

In order to verify the effectives of a friction compensator and a disturbance observer with SMC in energy saving, consumed energy and control variance for each axis were also calculated experimentally. The former was measured using a power Hi-tester (HIOKI 3334AC/DC) that is installed between a motor driver and a motor to measure energy consumed by a motor directly, while the latter was calculated using the following equation.

$$\sigma_i = \sqrt{\frac{\sum_{j=1}^{J}(f_{cij} - \Theta_i)^2}{J}} \qquad i = x, y \tag{22}$$

where Θ_i, f_{cij} are the mean of all control signals and the control signal value at the j^{th} sampling instant of the i^{th} axis, respectively. J is the total number of sampling instants ($j = 1, 2, ..., J$). The consumed energy was reduced by 2.76% and 3.01% for X and Y axis as shown in Fig. 7, respectively. Figure 8 compares control variance for SMC and SMCFD in X and Y axis, respectively. Although the control input variance of X axis was increased by 3.07% and weakly affected by the motor driver, control variance of Y axis was largely reduced by 14.13%.

The ASMC was also integrated with the same nonlinear friction and disturbance observer. The control gain of ASMC is automatically tuned depending on the resultant contour error to generate appropriate control signal. The ASMCFD can achieve a better performance by minimizing the tangential and normal errors as well as the actual contour error compared to ASMC and additionally improved the tracking errors as shown in Fig. 9. Figure 10 demonstrates significant improvement in the mean and maximum contour

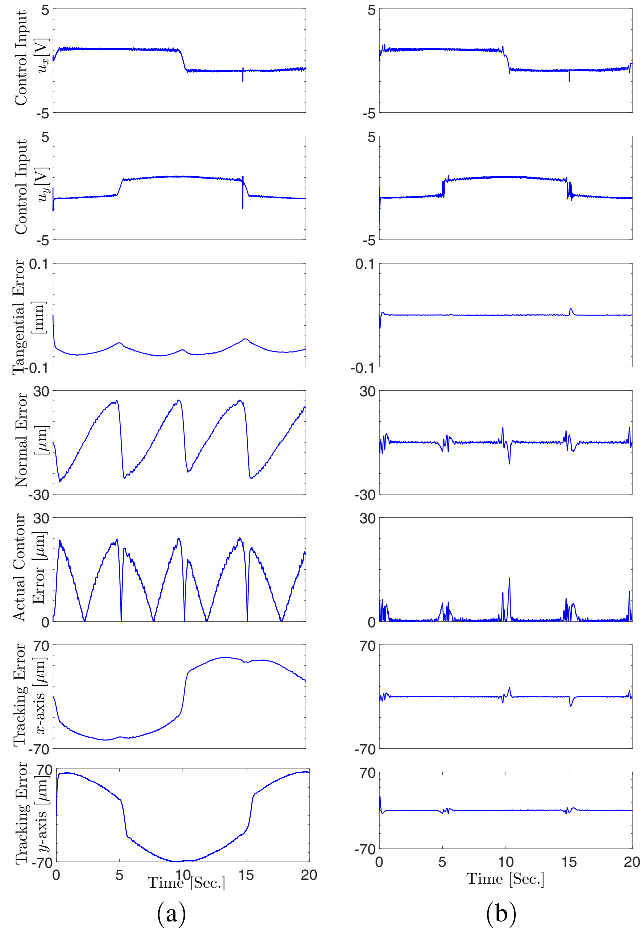

Fig. 4. Experimental Results: (a) SMC and (b) SMCFD.

TABLE I
CONTROL PARAMETERS

Parameter	Value	Parameter	Value
λ[s^{-1}]	diag{10,20}	K_c[s^{-1}]	20
β [−]	diag{1.5,1.7}	ρ[mms^{-1}]	40
η_{t_m}[s^{-1}]	10	k_p[s^{-2}]	3500
η_{n_m}[s^{-1}]	10	k_d[s^{-1}]	150
k_{t_m}[mm^{-1}]	10	k_{ev}[s^{-1}]	40
k_{n_m}[mm^{-1}]	50	k_{ed}[kgs^{-1}]	50
δ[−]	0.01		

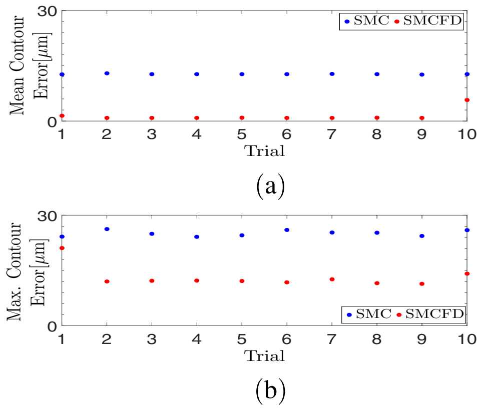

Fig. 5. Contour Errors for SMC and SMCFD: (a) Mean and (b) Maximum.

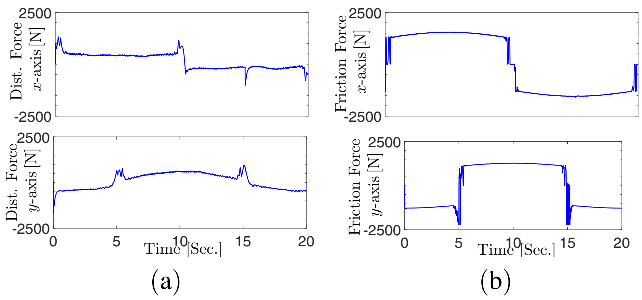

Fig. 6. Estimated Forces for SMCFD: (a) Disturbance and (b) Friction

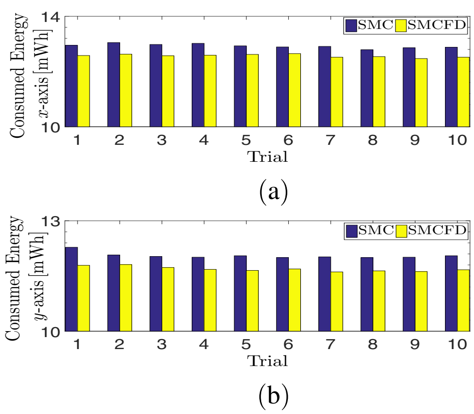

Fig. 7. Consumed Energy: (a) X-axis and (b) Y-axis.

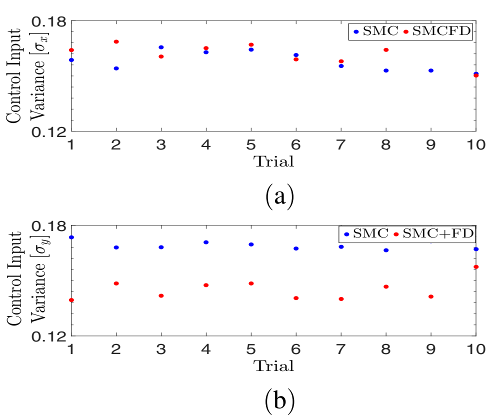

Fig. 8. Control Input Variance for SMC and SMCFD: (a) X-axis and (b) Y-axis.

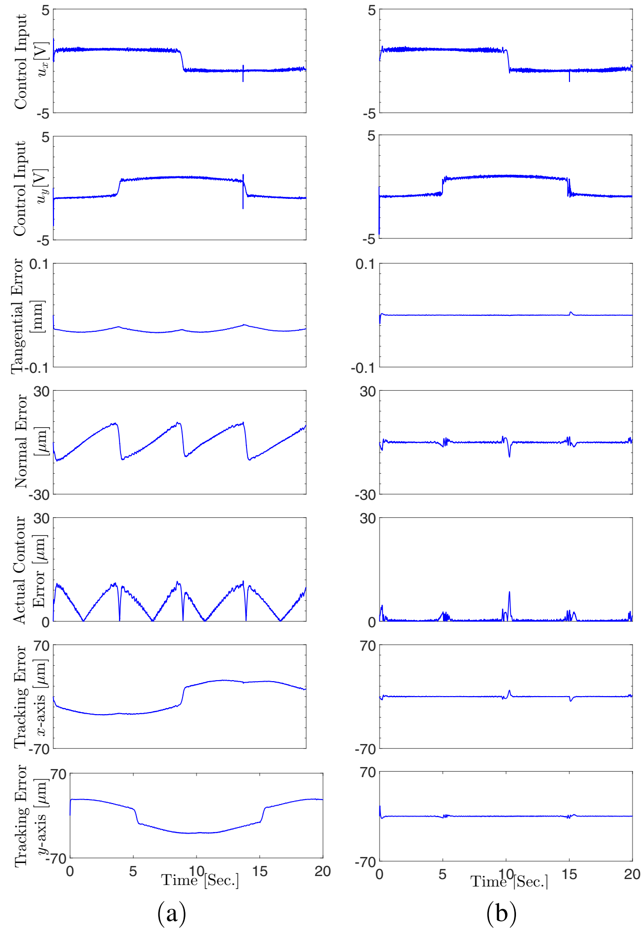

Fig. 9. Experimental Results: (a) ASMC and (b) ASMCFD.

errors in which they were decreased by 91.72% and 38.6%, respectively. The disturbance and friction forces are shown in Fig. 11. Figure 12 confirmed the effectiveness of the proposed approach for reducing consumed energy by 0.898% and 2.05% for X and Y axis, respectively. Although the control input variance was increased by 1.15% for X axis, it was reduced for Y axis by 2.86% as shown in Fig. 13.

V. CONCLUSIONS

In this paper, the nonlinear friction model and disturbance observer have been combined into SMC and ASMC based on the authors' previous work [13]. The proposed approach can largely improve the contouring performance of a biaxial feed drive system and reduce the consumed energy. In the SMCFD, the mean and maximum contour errors were highly reduced by 88.98% and 47.76%, respectively. The consumed energy was decreased by 2.76% and 3.01% for X and Y axis, respectively.

In the ASMCFD, the mean and maximum contour errors were reduced by 91.72% and 38.6% compared to using only ASMC, respectively. The consumed energy was also reduced by 0.898% and 2.05% for X and Y axis, respectively. Future work includes application to three axis machining for energy saving.

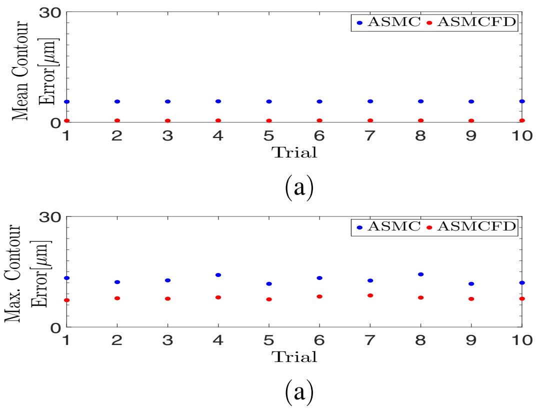

Fig. 10. Resultant Contour Errors for ASMC and ASMCFD: (a) Mean and (b) Maximum.

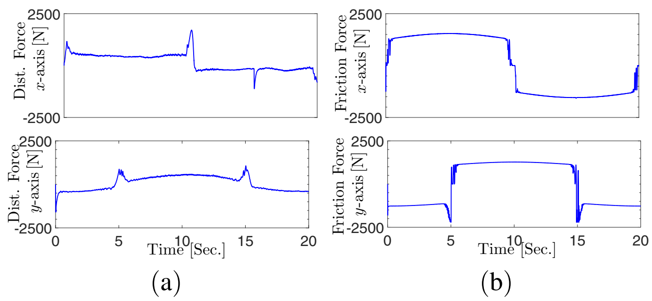

Fig. 11. Estimated Forces for ASMCFD: (a) Disturbance and (b) Friction.

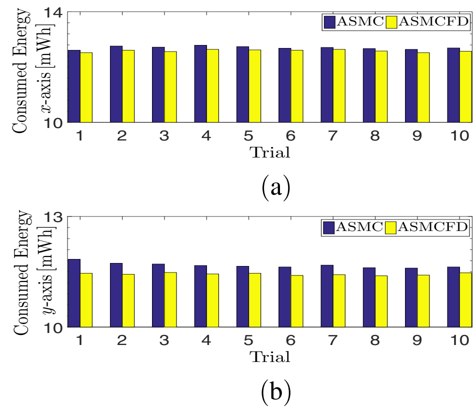

Fig. 12. Consumed Energy: (a) X-axis and (b) Y-axis.

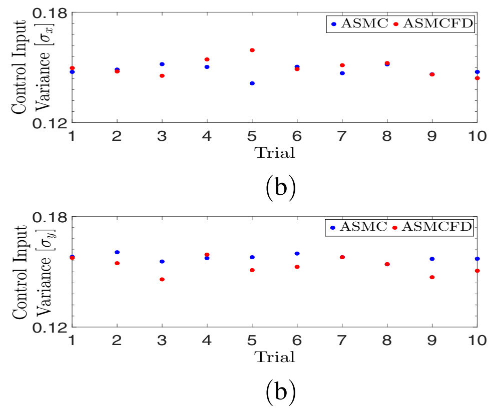

Fig. 13. Control Input Variance for ASMC and ASMCFD: (a) X-axis and (b) Y-axis.

REFERENCES

[1] B. Armstrong-Hlouvry, P. Dupont, and C. Canudas. "A survey of models, analysis tools and compensation methods for the control of machines with friction." *Automatica*, Vol. 30, No. 7, pp. 1083-1138, 1994.

[2] W. Lee, C. Lee, and B. Min. "Simulation-based energy usage profiling of machine tool at the component level." *Int. J. of Precision Engineering and Manufacturing-Green Technology*, Vol. 1, No. 3, pp. 183-189, 2014.

[3] Dahl, Phil R. "A solid friction model." *Aerospace Corp El Segundo Ca*, 1968.

[4] W. Lee, C. Lee, Y. Jeong, and B. Min. "Friction compensation controller for load varying machine tool feed drive." *Int. J. of Machine Tools and Manufacture*, Vol. 96, pp. 47-54, 2015.

[5] C. Lin, and C. Lee. "Observer-based robust controller design and realization of a gantry stage." *Mechatronics*, Vol. 21, No. 1, pp. 185-203, 2011.

[6] C. Kempf and S. Kobayashi. "Disturbance observer and feedforward design for a high-speed direct-drive positioning table." *IEEE Trans. on Control System Technology*, Vol. 7, No. 5, pp. 513-526, 1999.

[7] Ba. Bui, N. Uchiyama, and S. Shigenori. "Nonlinear friction modeling and compensation for precision control of a mechanical feed-drive system." *Sensors and Materials*, Vol. 27, No. 10, pp. 971-984, 2015.

[8] D. Kamalzadeh and K. Gordon. "Robust compensation of elastic deformations in ball screw drives." *Int. J. of Machine Tools and Manufacture* , Vol. 50, No. 6, pp. 559-574, 2010.

[9] C. Lin, H. Yau, Y. Tian. "Identification and compensation of nonlinear friction characteristics and precision control for a linear motor stage." *IEEE/ASME Trans. on Mechatronics*, Vol. 18, No. 4, pp. 1385-1396, 2013.

[10] A. Keck, J. Zimmermann, and O. Sawodny. "Friction parameter identification and compensation using the elastoplastic friction model." *IEEE/ASME Trans. on Mechatronics*, 2017.

[11] Y. Koren. "Cross-coupled biaxial computer control for manufacturing systems", *ASME J. Dynamic Systems, Measurement, and Control*, Vol. 102, No. 4, pp. 265-272, 1980.

[12] A. Khalick and N. Uchiyama. "Contouring controller design based on iterative contour error estimation for three-dimensional machining." *Robotics and Computer-Integrated Manufacturing*, Vol. 27, No. 4, pp. 802-807, 2011.

[13] A. Farrage and N. Uchiyama. "Adaptive sliding mode contouring control with a nonlinear sliding surface for feed drive systems." *SICE Annual Conference*, pp. 230-235, 2017.

[14] C. Peng and C. Chen. "Biaxial contouring control with friction dynamics using a contour index approach." *Int. J. of Machine Tools and Manufacture*, Vol. 47, No. 10, pp. 1542-1555, 2007.

[15] N. Rafan, Z. Jamaludin, T. Chiew, L. Abdullah, and M. Maslan. "Contour error analysis of precise positioning for ball screw driven stage using friction model feedforward." *Procedia CIRP*, Vol. 26, pp. 712-717, 2015.

[16] N. Uchiyama, "Contouring control of biaxial feed drive systems with non-linear friction compensation." *Proceedings of the Institution of Mechanical Engineers, Part I: Journal of Systems and Control Engineering*, Vol. 222, No. 3, pp. 153-162, 2008.

[17] Ba. Bui and and N. Uchiyama. "Sliding mode contouring controller design with adaptive friction compensation for three-axis machine tools." *IEEE American Control Conference*,pp. 2217-2222, 2016.

[18] Y. Su, D. Sun, and B. Duan. "Design of an enhanced nonlinear PID controller", *Mechatronics*, Vol. 15, No. 8, pp. 1005-1024, 2005.

[19] A. Khalick, N. Uchiyama, and S. Shigenori. "Energy saving in feed drive systems using sliding-mode-based contouring control with a nonlinear sliding surface", *IEEE/ASME Trans. on Mechatronics*, Vol. 20, No. 2, pp. 572-579, 2015.

[20] A. Merabet, R. Beguenane, J. Thongam, and I. Hussein. "Adaptive sliding mode speed control for wind turbine systems." *IEEE Annual Conf. on Industrial Electronics Society*, pp. 2461-2466, 2011.